Active Polymeric Composite Membranes for Localized Actuation and Sensing in Microtransfer Printing

Numair Ahmed, Canan Dagdeviren, John A. Rogers, *Fellow, IEEE*, and Placid M. Ferreira

***Abstract*— Soft locally active structures are becoming increasingly important in a number of applications, from microfluidic systems to soft robotics. In this paper, we develop an active polymeric composite membrane for use as an active stamp in the microtransfer printing process. The membrane is a composite of multiple layers: 1) a soft polydimethylsiloxane layer for transfer printing; 2) a lead zirconate titanate ($PbZr_{0.52}Ti_{0.48}O_3$) layer for actuation; 3) metal layers for strain sensing and interconnects; and 4) patterned photopolymer (SU-8) layers for selectively tuning the compliance in the membrane and for handling. A novel and scalable fabrication approach that uses photolithography and microtransfer printing is developed for heterogeneously integrating the different materials into a functional structure. Approaches to designing and characterizing these active membranes are also discussed. Finally, the use of such membranes as stamps in the microtransfer printing process is demonstrated. By distributing actuation closer to critical regions of the tool, adaptability to local conditions for increased robustness and greater process flexibility is achieved. [2014-0211]**

***Index Terms*— Microactuators, microassembly, micromachining, microelectromechanical devices, transfer printing, active composite.**

I. Introduction

RECENT years have seen an increasing trend towards compliant structures and the use of soft materials for active mechanical devices. Bio-mimetic and soft robotic designs that use soft and deformable structures to deal with uncertain and dynamic environments such as physical contact and manipulation are good examples of this trend. However, from a mechanical design perspective, it is challenging, if not sometimes impossible, to transmit transient, small and precise forces and motions across long distances through such soft materials at the speeds and precision demanded by the application. Therefore, it becomes necessary to integrate such mechanical functions into the soft materials as close as possible to the location where they are needed. This raises interesting challenges for engineering, design, materials selection and compatibility, and fabrication. Novel microscale sensor, actuator, power source technologies, new device classes for flexible electronics, and new materials and fabrication/manufacturing technologies offer new pathways for realizing such soft mechanical devices [1]. For example, organic semiconductors and conducting polymers, with their inherent flexibility and low stiffness have been considered attractive materials for embedding flexible, stretchable, large area electronic [2], [3] and sensing capabilities in such soft systems. Further, the exploitation of atypical mechanical behaviors of high-quality mono-crystalline inorganic semiconductor materials at lower dimensions and small scales - such as micro/nano wires, ribbons and membranes – has also been demonstrated as feasible pathways for similar capabilities [4]–[8]. The latter approach to heterogeneous integration with well-characterized and optimized material sets allows for the development of novel devices with tight integration of mechanical, optical, electronic and fluidic functionality without sacrificing performance.

In this work, we present a novel pathway to the realization of soft, but active composite membranes by embedding micro-scale piezoelectric lead zirconate titanate (PZT) thin film actuators and metallic strain gages into polymeric films. The inherent processing conditions (high temperatures) required for PZT make it incompatible with many polymers. A key manufacturing step in overcoming this challenge is micro-transfer printing [9], and self-referentially, these active membranes are motivated by the need to develop micro-transfer printing stamps with local actuation and sensing capabilities for enhanced process robustness and flexibility.

In this paper, we design, fabricate and test active polymeric membrane stamps for micro-transfer printing. These active membrane stamps have PZT actuation and strain gage deflection/force sensing at each printing site or 'post' of the stamp. The structure developed here is motivated by and applied to a micro-manufacturing assembly process. However, the heterogeneous integration architecture and the design and fabrication approach are easily transferrable to other applications such as microfluidic systems, micro-robotic swimmer and active substrates for cell manipulation. The paper is arranged in the following sections; first the context and motivation, here the micro-transfer printing process is given; next, the design of

Manuscript received July 15, 2014; revised October 26, 2014; accepted November 11, 2014. Date of publication December 17, 2014; date of current version July 29, 2015. This work was supported by the National Science Foundation under Grant CMMI-0749028 and Grant CMMI-1301336. Subject Editor E.-S. Kim.

N. Ahmed is with the Department of Mechanical Science and Engineering, University of Illinois at Urbana-Champaign, Urbana, IL 61801 USA (e-mail: ahmed19@illinois.edu).

C. Dagdeviren is with the David H. Koch Institute for Integrative Cancer Research and McGovern Institute for Brain Research, Massachusetts Institute of Technology, Cambridge, MA 02139 USA (e-mail: dagdevi1@uiuc.edu).

J. A. Rogers is with the Department of Material Science and Engineering, Frederick Seitz Materials Research Laboratory and Beckman Institute for Advanced Science and Technology, University of Illinois at Urbana-Champaign, Urbana, IL 61801 USA (e-mail: jrogers@illinois.edu).

P. M. Ferreira is with the Department of Mechanical Science and Engineering, University of Illinois at Urbana-Champaign, Urbana, IL 61801 USA, and also with MEMS Solution Inc., Yongin 135-280, Korea (e-mail: pferreir@illinois.edu).

Color versions of one or more of the figures in this paper are available online at http://ieeexplore.ieee.org.

Digital Object Identifier 10.1109/JMEMS.2014.2375811

1057-7157 © 2014 IEEE. Personal use is permitted, but republication/redistribution requires IEEE permission.
See http://www.ieee.org/publications_standards/publications/rights/index.html for more information.

the proposed membrane including the architecture and finite element analysis is introduced; the fabrication of the proposed active membrane devices is described along with testing of the actuation and sensing capabilities; finally, the active membrane stamp is used to demonstrate device manipulation within the micro transfer printing process and conclusion are drawn.

II. Context and Motivation

Micro-Transfer Printing is a micro-scale assembly process for transferring prefabricated micro and nano scale functional devices fabricated in dense arrays on native growth/fabrication substrates (such as silicon, germanium, sapphire or quartz) to a broad range of functional receiving substrates such as polymers, cloth, biocompatible silks, electro-active paper etc. to realize novel devices such as wearable electronics, conformal bio-compatible sensors and many more [4], [10], [11] with any desired aerial density. The process has also been demonstrated for the creation of electrically tunable microcavities [12] MEMS actuator and sensor assembly [13] and patterning of metal conductors on polymeric substrates [14]. The process has been implemented industrially to assemble concentrated photovoltaic modules [15], [16] and integrated circuits [17]. A variation of the process has also been demonstrated in printing carbon nanotubes and creation of carbon-nanotube based field effect transistors [18], [19]. Micro-contact printing can be thought of as belonging to the family of transfer printing processes, and in the context of working with liquid inks, such process have be used for printing small amounts of liquid drug solutions in micro cavities [20] and printing biological fluids and proteins for analysis [21] and printing full-color quantum dot displays [22].

Central to the process is a molded polydimethylsiloxane (PDMS) stamp, patterned with microscale posts. The patterned posts allow for selective engagement of the stamp to pre-fabricated micro structures on a donor substrate. These microstructures (referred to as 'ink'), are typically fabricated by conventional (lithography-based) microfabrication processes on a sacrificial layer that, after the device or ink fabrication is completed, is undercut etched to leave the devices tethered to the donor substrate by specially designed anchors that are engineered to fail during the printing process. Strong van der Waal interactions between the PDMS and the surface of the ink are responsible for adhesion of the ink to the stamp and their subsequent release from the donor substrate during retrieval, by peeling them off with the help of the stamp. Printing occurs when the 'inked' stamp is later brought into contact with a target substrate, followed by slowly retracting the stamp. Precise control of separation velocity is used to exploit the rate-dependent adhesion of the viscoelastic-elastic stamp-ink interface to enable the release of the ink from the stamp [9], [23]–[25]. The use of a patterned stamp allows engagement with any desired set or pattern of devices on the donor; thus permitting printing of any desired pattern or areal density into a functional substrate. Figure 1 shows a schematic of the printing process, showing important process events and depicting important stamp features. It also shows micrographs of how ink are sequentially retrieved from densely packed donor substrates and spread onto the receiving substrate. Finally, the figure shows detailed Scanning Electron Microscope (SEM) images of a typical micro-fabricated ink that is undercut etched while still anchored to the donor substrate, the same region after ink retrieval and the ink printed onto the target substrate, taken from [26].

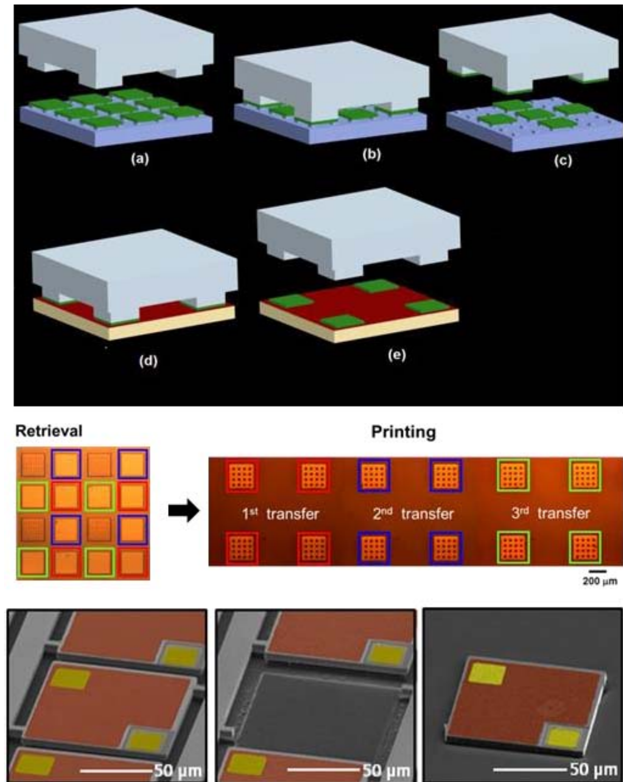

Fig. 1. (top) Representation of transfer printing using a patterned stamp with 4 posts, showing the individual process steps: (a) Translation and alignment to donor wafer. (b) Selective engagement with ink. (c) Ink retrieval from donor wafer. (d) Contact with acceptor substrate. (e) Device release onto acceptor substrate, (middle) results of 3 printing cycles show how ink from a dense donor substrate is expanded on a receiving substrate, and (bottom) SEM images of representative micro-LED, shown in sequence, (left) donor substrate before retrieval (center) after retrieval from the donor substrate, and (right) after transfer-printing onto a receiving substrate [26].

High throughput is achieved by increasing the number of microstructures transferred in each print cycle (see Figure 1). This necessarily means more printing posts and larger stamp areas. As the printing parallelism increases, it becomes increasingly challenging to monitor and control what happens at a single post, leading to a general loss of robustness of the entire process. Small misalignments between the substrate and the stamp can get magnified by the dimensions of the stamp and lead to significant variations in the printing conditions at posts in different areas of the stamps, resulting in local printing failures. Additionally, failure to print a microstructure in one cycle at a particular post can result in repeated failures at the same post in subsequent cycles. Variability and non-repeatability in printing can also arise when large receiving substrates are involved, as a result of their flatness and waviness. Additionally, with receiving substrates being quite large (several 10's of centimeters) and with devices often sparsely distributed on the substrate, i.e., with large area expansions (for concentrated photovoltaic applications, for example), the stamp can have lateral dimensions of several centimeters,

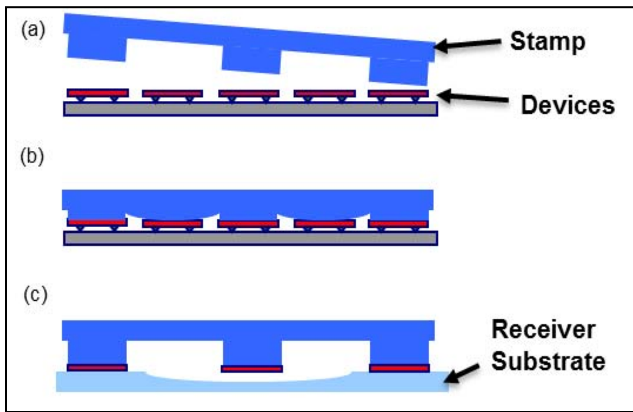

Fig. 2. Schematic representation of some failure modes encountered during transfer printing process. (a) Angular misalignment of stamp. (b) PDMS stamp collapse. (c) Acceptor substrate defect (waviness/bowing).

with posts whose dimensions are in 10 to 500 micrometer range, distributed at a pitch of several millimeters. This makes the stamp susceptible to collapse [27], [28] especially when large printing forces are used to compensate for misalignments between the stamp and the substrate. Such collapses, when they occur on the donor substrate, damage it by peeling out microstructures wherever contact occurs. Some of these failure modes are shown schematically in Figure 2.

In addition to failure modes, situations requiring selective device pick up, printing, collection and sorting; such as a donor substrate with known failed devices or devices with varying performance grades, devices requiring pick up from, or printing onto multiple substrates are application areas where selective control of stamp geometry can be especially valuable. It is therefore important to explore strategies to monitor and adjust the process at the scale of individual posts on the stamp. Hence, there is a strong drive to move from bulk, passive PDMS stamps to active stamps. Active stamps provide precisely this capability, creating a strong motivation to migrate away from the use of passive, bulk PDMS stamps currently used by the process. Our previous research [29]–[31] has addressed the issue of monitoring the process at the resolution of a single post. A composite, multi layered stamp was developed with an embedded strain gage behind the printing post so that the forces during the print cycle could be monitored. Further, it was shown that a statistical classifier could use the force signals to identify printing or pickup failures at the posts.

In this paper, we address the problem of adjusting the process by making the stamp active with actuators capable of moving each printing post. In the next section, we introduce the idea of an active, layered composite membrane and, using the requirements of the micro-transfer printing process, design an active array of printing posts on a PDMS web with a patterned backing or support layer to provide it with tailored compliance. The design and fabrication of the stamp are discussed in detail.

III. Design of Active Membrane Composite Stamps

The driving motivation in the design of the active membrane composite stamp is to preserve the local process conditions for successful transfer printing, while providing the stamp with the capability to adjust its geometry to compensate for local deviations from nominal geometry of the donor and receiver substrates, thus providing for process robustness. Additionally, with local actuation capabilities, the stamp is able to provide process flexibility, permitting selective pick up or printing of microstructures in any pattern by appropriately actuating selected posts. This requires the integration of many different functions into the membrane, namely, a functional material for microstructure pick-up and release during micro-transfer printing, actuators for producing force/motion at the posts and sensors for measuring the force or the deflection, interconnects for bringing in power and extracting signals and structures for tuning the compliance to localize and direct the deformations in the membrane. From a design methodology perspective, we assign each function to a different layer within the composite. Figure 3 shows a solid model of the composite membrane with the various layers providing the desired embedded functions. PDMS was chosen as the functional material because of previous experience with tuning its stiffness and adhesion properties for micro scale manipulation needed in micro-transfer printing [9], [23]. The PDMS layer is patterned with posts to replicate the geometry of a conventional micro-transfer printing stamp. The actuation is provided by a piezo-electric PZT layer that is first fabricated on a silicon growth substrate and then integrated into the polymer composite membrane using micro transfer printing. SU-8, an epoxy-based negative tone permanent photoresist is used as the compliance tuning layer. Compliance at the printing posts is achieved by patterning cantilevers in this layer. The embedded sensor is a strain gauge integrated into the cantilever. A metallization layer for interconnects is below this layer. Finally, the stamp is completed with a thick handle layer made of SU-8 and patterned with windows to permit unrestricted deflection of the cantilevers and optical viewing from above the stamp (required for alignment and registration).

The above selection of materials is based on function, but also compatibility with the fabrication strategy (described later). With this selection of materials, the dimensions i.e. thickness of the layers and lateral dimensions of features such as the cantilevers and the PZT actuators, the location of the PZT actuator relative to the cantilever and the PDMS post can be arrived at by using finite element analysis (FEA). The dimensions of the PZT membrane and the dimensions of the cantilevers were calculated using the FEA. Fabrication constraints on the thickness and dimensions of the layers in the composite were also considered to create a search space; from which appropriate dimensions to obtain a minimum stiffness and deflection of 150 N/m and 5 μm, respectively at the printing posts were arrived at. Based on fabrication constraints the thickness of the PDMS layer and the location of the PZT layers were constrained. The thickness of the PDMS layer was set at 20 μm which is the thinnest layer that can be reliably spun coated while having PDMS posts with dimensions of 250 μm $\times$ 250 μm, 100 μm tall. The thickness of the sol-gel based PZT film was determined by the availability[1] of

[1]MEMS Solution Inc., Korea.

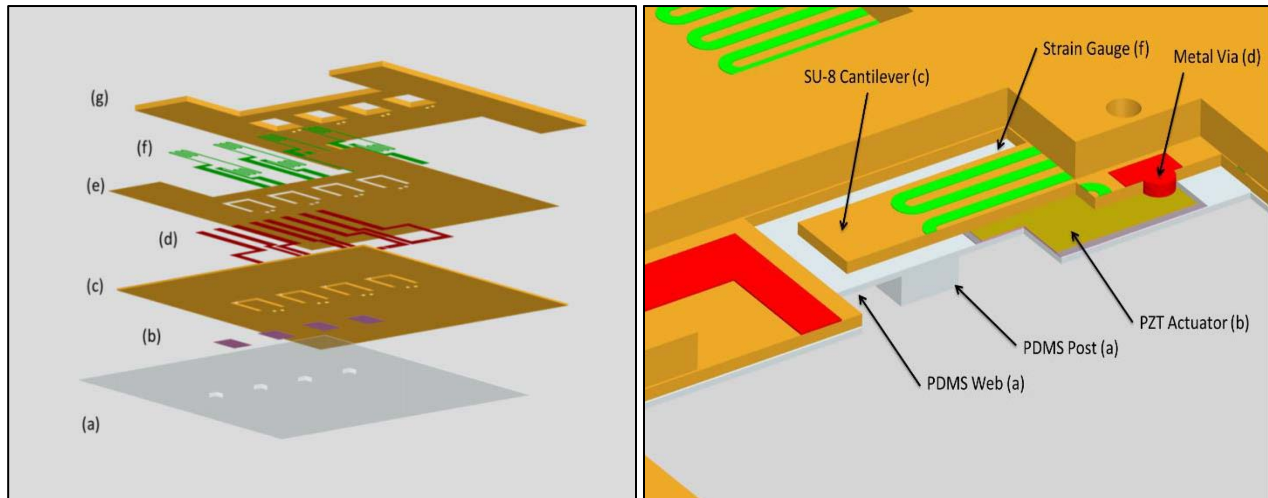

Fig. 3. (Left) Exploded view of the solid model of the device showing the individual layers. (a) PDMS layer with posts, (b) PZT thin film placed for embedding actuation, (c) SU-8 structural layer providing selective compliance, (d) Metal interconnects, (e) SU-8 Encapsulation layer, (f) Metal strain gauge, compensation gauge and interconnects, (g) Handle layer. (Right) Close up view of a single post of active membrane composite stamp showing the integration of the individual functional layers.

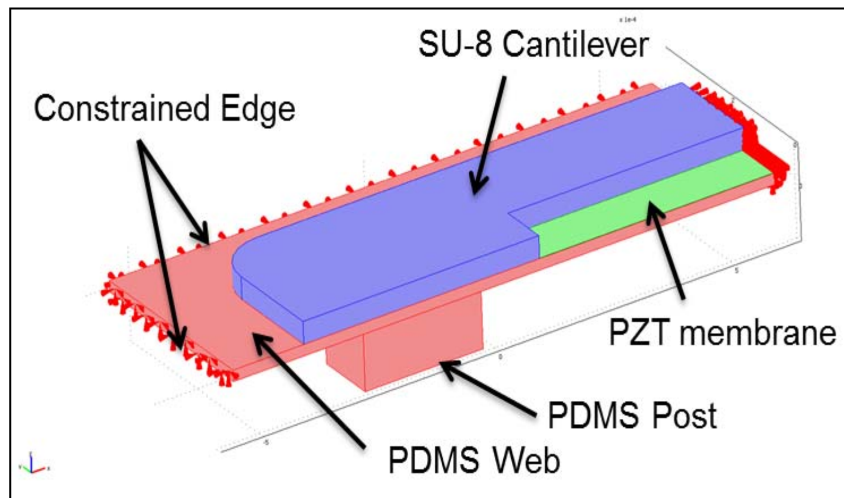

Fig. 4. Isometric view of a half section of the FEA model, showing the PDMS web and post, the SU-8 cantilever, location of the PZT membrane and the constrained edges of the PDMS web.

Silicon wafers with appropriate thin film layers (namely Platinum, PZT and Silicon Dioxide). A 0.5 μm thick PZT layer is embedded into the SU-8, at the SU-8/PDMS interface. The location of the PZT within the composite membrane was constrained by micro transfer printing requirements. The PZT actuator has bottom platinum and top gold layers, forming the two electrodes and need to be accessed for the purpose of supplying power. For a piezoelectric sheet, the poling direction (usually along the thickness) is designated as the 3-axis with axes 1 and 2 in the plane of the sheet. If the piezoelectric coefficients defining strain per unit electric field at constant stress are d_{ij}, then d_{31}, d_{32} and d_{33} represent the normal strain induced in the 1, 2 and 3 direction respectively, due to an electric field applied in the poling direction. Assuming transverse isotropy we have $d_{32} = d_{31}$. PZT based actuation of a cantilever structure can be characterized into two categories, namely longitudinal or d_{33} and transverse or d_{31} type; depending upon the direction of applied field and resulting strain. In a d_{33} type cantilever, an in-plane electric field induces an in-plane strain, which contracts or expands the PZT material [32], [33]. In a d_{31} type cantilever, the applied electric field is normal to the cantilever and the in-plane expansion or contraction is used to generate deflection of the cantilever. The former (d_{33}) requires the use of two metal interdigitated electrodes (IDE) on top of the piezoelectric film [34], while the latter (d_{31}) uses two sheet electrodes on the top and bottom of the piezoelectric film. Given the configuration of the PZT films, described above, our work uses the d_{31} actuation mode.

A three dimensional multiphysics based FEA model of a single cantilever was made to calculate the required dimensions of the various layers to meet design requirements. The FEA was done using the Piezosolid application mode within the MEMS module of COMSOL Multiphysics® software (version 3.5a). An image of the model geometry is shown in Figure 4. The bottom most layer in the model is a 20 μm thick layer of PDMS with a 250 μm × 250 μm, 100 μm tall post, forming the PDMS membrane, the edges of the membrane are

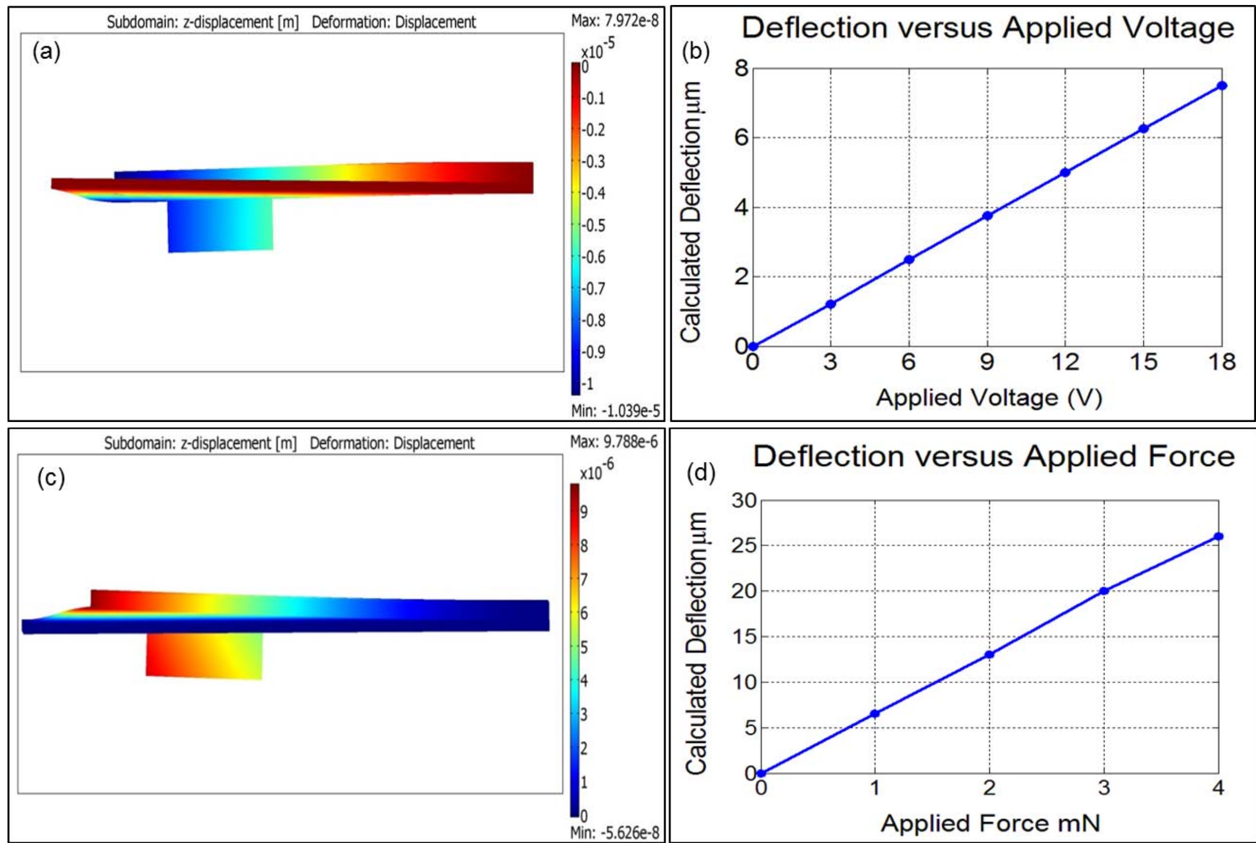

Fig. 5. Results of FEA performed to calculate stamp deflection under actuation and applied forces. (a) Representative FEA computed deflection under actuation. (b) Graph of computed deflection at the post for various applied actuation voltages. The maximum deflection is 7.5 μm. (c) Representative FEA computed deflection when a force is applied at the post. (d) Calculated deflection at the post for various applied forces. The calculated stiffness is 150 N/m.

constrained to be fixed. The dimensions of the membrane are to be determined. A 0.5 μm thick layer of PZT is bonded on top of the PDMS membrane. The lateral dimensions of this membrane are to be determined. The next layer of the model is an SU-8 layer, forming the cantilever. The SU-8 cantilever is bonded to the PZT and PDMS. The base of the SU-8 cantilever is constrained. The final dimensions of the cantilever are to be determined using FEA. The elastic modulus of SU-8 used in the simulation was 4.02 GPa [35], the elastic modulus for PDMS was 2.0 MPa, and the PZT material properties such as the compliance, piezoelectric coupling used in the simulation were that of PZT-8 [36].

In the search for appropriate dimensions, first a force was applied to the face of the PDMS post, with no voltage applied across the PZT (top and bottom surface of the PZT were given ground electrical boundary conditions). The deflection of the cantilever and post under applied load was calculated, the thickness of the SU-8 layer in the composite and the lateral dimension of the cantilever and PDMS web were varied to get the desired stiffness. Next, voltage was applied to the PZT and deflection of the cantilever and post was calculated. The dimension of the PZT, SU-8, and PDMS were again varied to achieve the desired deflection and the iterations were continued until both design criteria were met. Constraints such as limitation on dimensions originating from fabrication processes were considered throughout the design process.

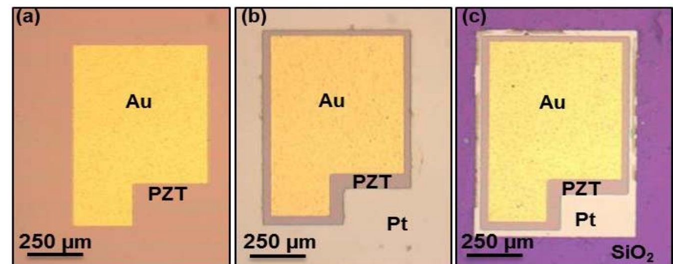

Fig. 6. Fabrication of PZT ink for transfer printing. (a) Gold patterning after deposition. (b) PZT etching. (c) Pt etching.

The dimensions of the PDMS web, the PZT membrane, and the SU-8 cantilever were calculated to be a length of 1000 μm and a width of 900 μm, a width of 600 μm and a length of 500 μm, and a width of 650 μm, a length of 900 μm respectively. The thickness of the SU-8 cantilever was calculated to be 40 μm. Figures 5(a) shows a typical profile of the stamp when actuated and Figure 5(b) shows the FEA computed stamp deflections (at the face of the post) as a function of applied actuation voltages. A maximum deflection of about 7.5 μm at the face of the PDMS post is predicted for an applied voltage of 18V with an actuation constant of 0.417μm/V. A typical deflection profile of the stamp when a force is applied at the post is shown in Figure 5(c), while Figure 5(d) shows the computed deflection at the post as

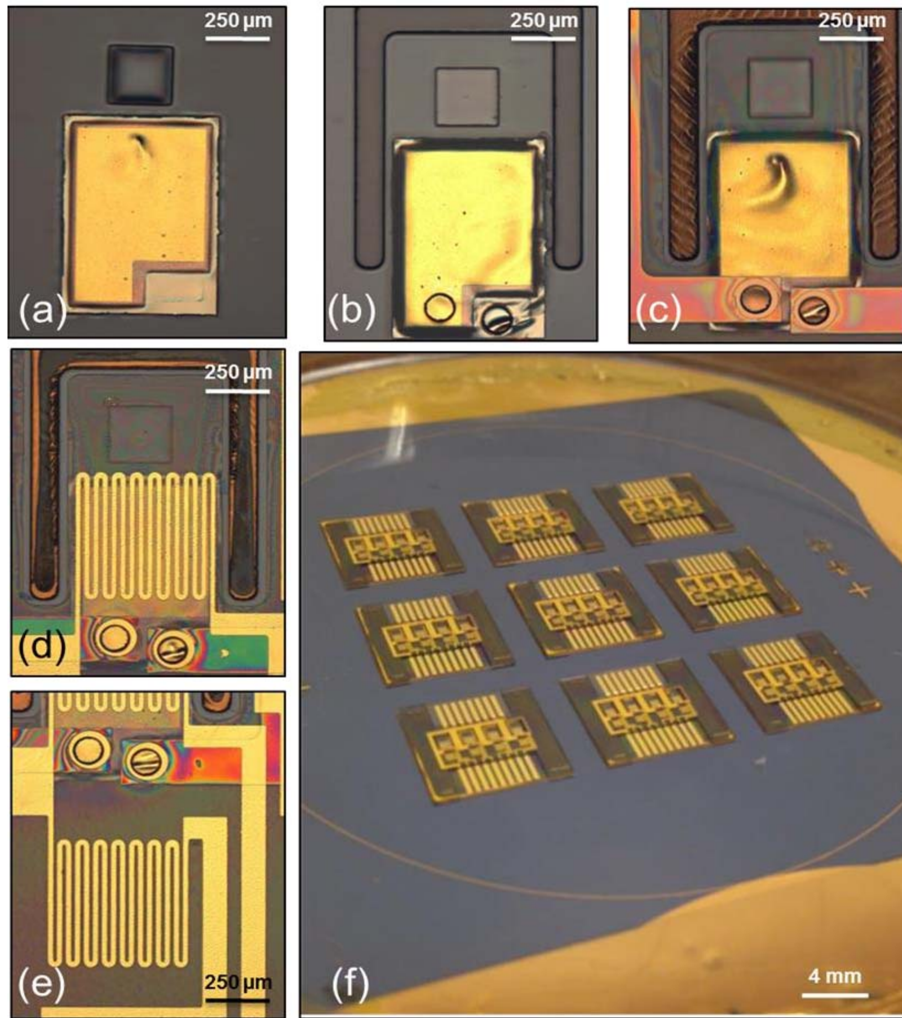

Fig. 7. Fabrication of the active membrane composite stamp. (a) PZT actuator ink transfer printing. (b) SU-8 structural layer photolithography. (c) First metal interconnect layer formation and passivation. (d) Second metal layer fabrication forming the sensing and (e) compensation strain gauges and interconnects. (f) Image of a single wafer with nine individual stamps.

a function of the applied force. The stiffness of the overall composite stack can be observed to be about 150 N/m for the designed dimensions.

IV. Fabrication

This section presents the details of the fabrication process used to create the PZT ink, and the active composite membrane stamp. All processes were done at a temperature of 75 °C to reduce thermally induced internal stresses [37].

A. PZT Ink Fabrication

The individual PZT elements, embedded into the composite membrane stamp, consists of a layer of PZT (500nm) sandwiched between a top (Au/Cr, 200nm/5nm) and a bottom (Pt/Ti, 200nm/20nm) electrode. The dimensions of each PZT element are $600 \times 900\ \mu m^2$, slightly longer than the value calculated from the FEA to allow for placement of contacts. These PZT elements, are fabricated from a multilayer stack of $Pb(Zr_{52}Ti_{48})O_3/Pt/Ti/SiO_2$ (500nm/200nm/20nm/600nm) thin films on Si (100) wafer (MEMS Solution Inc.). The top electrode is composed of 200 nm thick gold on top of 5 nm thick seed layer of chromium, deposited by Electron Beam Physical Vapor Deposition on the PZT surface. After deposition of gold top electrode, the PZT is poled at 150 °C using a 100 kV/cm electric field, applied normal to the plane of the PZT for 1 hour.

After poling, the multilayer structure is patterned into arrays of individual units for use in micro transfer printing. This step of creating arrays of micro structures for micro transfer printing is referred to as "ink" fabrication. First the top electrode is patterned using a photoresist (AZ4620) etch mask; patterned using photolithography. This is followed by etching of the gold layer by gold etchant (Transene Company Inc., TFA), and chromium layer by CR-7 chrome etchant (OM Group, USA), respectively. Similarly the PZT and Platinum are patterned by etching in a 4.5:4.5:91 v/v solution of HNO_3 (Nitric Acid, 70%): Buffered Oxide Etch (BOE, 6:1): Deionized Water (H_2O), and a 4:1 v/v solution of Hydrochloric acid (HCl, 37%): Nitric acid (HNO_3, 70%) at 95 °C, respectively [38].

After the individual inks are fabricated, they are protected by photoresist (AZ4620) and undercut etched in 3:1 v/v

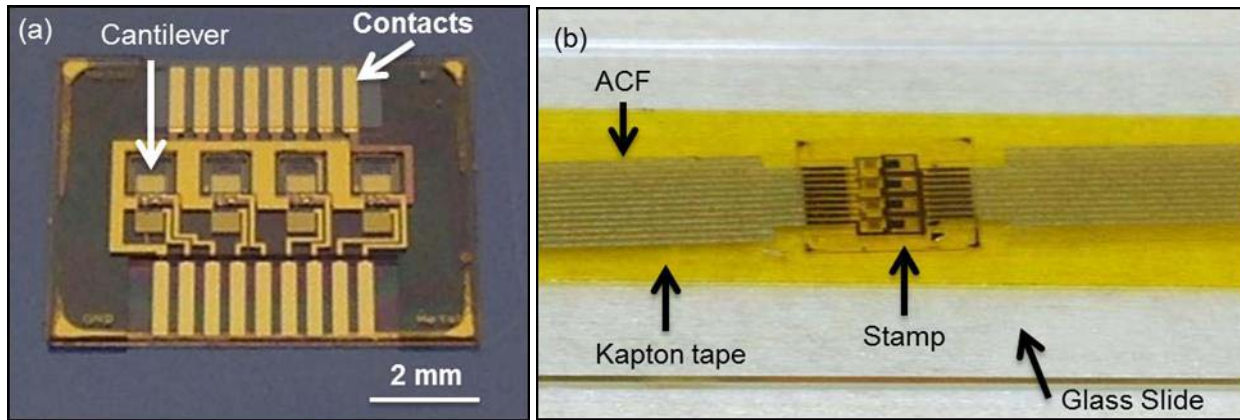

Fig. 8. (a) Image of a released stamp. (b) Image of a single stamp with array of four actuated posts attached to a glass slide with ACF connections.

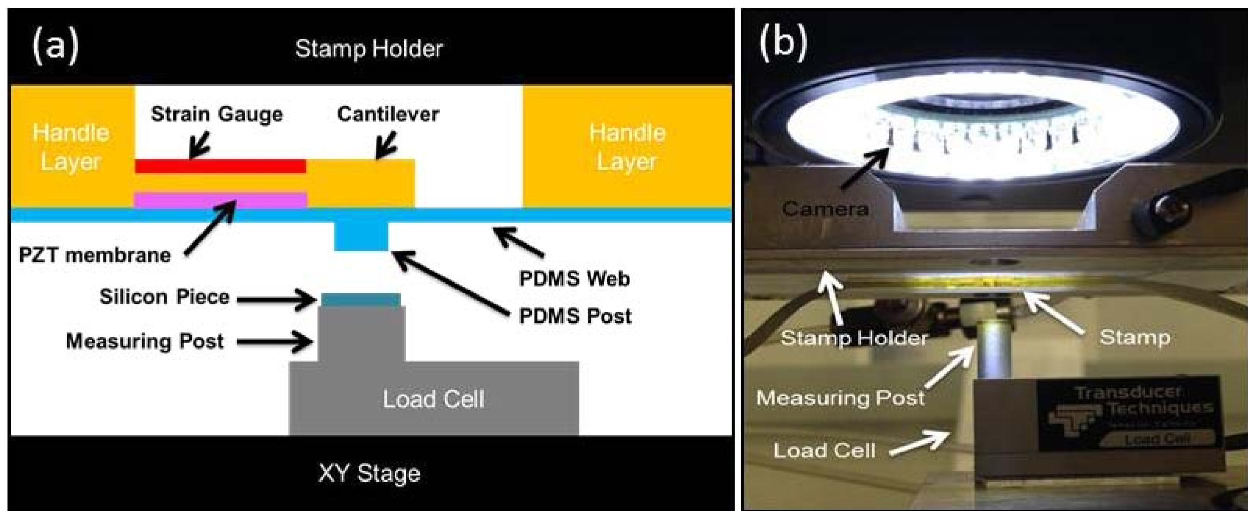

Fig. 9. (a) Schematic of the experimental setup used for characterization of the active membrane composite stamp. (b) Image of the experimental setup used for characterization of the active membrane stamp.

solution of Deionized Water (H_2O): Hydrofluoric acid (HF, 49%) for twenty minutes to partially undercut the Silicon Dioxide layer underneath the Platinum. This helps to release the ink from the edges (100 μm on each side) and allows them to be easily detached from the silicon substrate and transferred during transfer printing. Images of the individual fabrication steps are shown in Figure 6.

B. Active Membrane Composite Stamp Fabrication

This fabrication approach builds upon our previous work on the design and fabrication of composite stamps for micro transfer printing [30]. The first layer is a functional layer made of PDMS spun coated onto a mold to form a PDMS (20 μm thick) web that carries the posts. The active composite material; consisting of PZT and spin cast SU-8 (40 μm thick) is integrated on top of the PDMS followed by patterning the individual cantilevers and the die. Metal contacts (Ti/Cu, 10nm/500nm) and measurement and compensation metal strain gauges (Ti/Au, 10nm/50nm) are patterned on top of the SU-8. Finally a thick SU-8 (200 μm) layer is spun cast and patterned to form the handle layer of the stamp, providing rigidity for ease of handling and mounting.

Fabrication begins with the manufacturing of a SU-8 master mold, used to mold the PDMS layer. A 100 μm thick film of SU-8 50 (Microchem Corp.) is spun on to a polished silicon wafer and photolithographically patterned with square holes (for the printing posts on the PDMS layer). Before PDMS casting, the surface of the mold is coated with a thin layer of Polytetrafluoroethylene (PTFE), deposited using an Inductively Coupled Plasma Deep Reactive Ion Etching (ICP-DRIE) machine (PlasmaTherm, SLR 770) to prevent the PDMS from sticking to the mold and to facilitate eventual de-molding after fabrication is completed. A 20 μm thick PDMS (Dow Corning Corp., Sylgard 184) layer is spun coated onto the mold. The PDMS is semi cured in an oven at 70 °C for 30 minutes.

Metal-sandwiched PZT membrane 'inks' (whose fabrication was described earlier) are micro-transfer printed into specific locations on the semi-cured PDMS membrane, still on its SU-8 mold. Following the scheme depicted in Figure 1, a PDMS stamp with patterned posts is used to make contact with the PZT ink, extract them from the donor silicon handle substrate, and place them at predetermined locations on the PDMS membrane. Figure 7 (a) shows a close up of a single

PZT ink printed onto its target location. After transfer printing, the PDMS is fully cured at 70 °C for 24 hours in an oven. After fully curing, the PDMS surface is functionalized with a self-assembled monolayer (SAM) containing an amino group. To do this, the PDMS surface is first activated using an O_2 plasma in a Reactive Ion Etching (RIE) machine (March, CS-1701). Then the activated PDMS is soaked into a 1% v/v solution of (3-Aminopropyl)triethoxysilane (Sigma-Aldrich Corp., APTES) and methanol for 15 minutes, and then dipped in methanol for 2 minutes to desorb the excess APTES. This leaves behind a SAM on top of the PDMS which acts as an adhesion promoter for SU-8, facilitating SU-8 based micro fabrication on top of a PDMS substrate and permanently bonds the PDMS and SU-8 together, based on the reaction of the amino group of the SAM with the epoxy group of SU-8.

A 40 μm thick layer of SU-8 50 is spun coated on top of the PDMS/PZT, embedding the PZT into the polymer. The SU-8 layer is patterned to form the cantilever structures, once again using photolithography. The overlay registration is such that the posts in the PDMS are located under the free ends of the cantilevers. Thus, this layer provides the composite with selective compliance for locally actuating the printing posts. Via holes patterned in this layer allow for routing of electrical connections to the PZT actuator electrodes.

After fabrication of this layer, a 10 nm layer of Titanium followed by a 500 nm layer of Copper is sputtered using a vacuum sputtering tool (AJA International Inc., ATC Series). After sputtering, the contacts are formed by spin coating and patterning a photoresist (AZ 5214E) etch masks and etching the copper using copper etchant (Transene Company Inc., CE-100) and Titanium using BOE (Buffered Oxide Etch 6:1); forming the first level interconnects.

After the first level interconnects are patterned, a passivation layer of 5 μm thick SU-8 5 (Microchem Corp.) is spun coated and patterned. A layer of 10 nm thick Titanium followed by 50 nm thick Gold is sputtered on top of this passivation layer. After sputtering, the strain gauges used for sensing along with a co-located compensation resistor and their contacts are patterned by spin coating and patterning a photoresist (AZ 5214E) etch mask and etching the Gold and Titanium layers; forming the sensing layer in the composite, consisting of measuring strain gages, compensation gauge and interconnects.

After the sensing layer is formed, a 200 μm thick layer of SU-8 100 (Microchem Corp.) is spin coated and patterned to form the handle layer of the stamp forming individual dies, providing it with rigidity for ease of handling and mounting. Figure 7 shows micrographs of a single post and cantilever of the active membrane composite stamp during various stages of fabrication.

After fabrication the PDMS layer around the stamp die is cut, the individual dies are then released from the mold by separating the PDMS from the mold at one corner with a sharp blade and gently peeling it away from the mold. Figure 8(a) shows the image of a released die with an array of 4 actuated posts. After release from the fabrication substrate, Anisotropic Conductive Film (3M Corp., ACF) is bonded to the contacts and the membrane die is attached to a glass slide using double sided polyimide tape (Kapton tape), forming the final stamp. The image of a completed, interfaced stamp is shown in Figure 8(b).

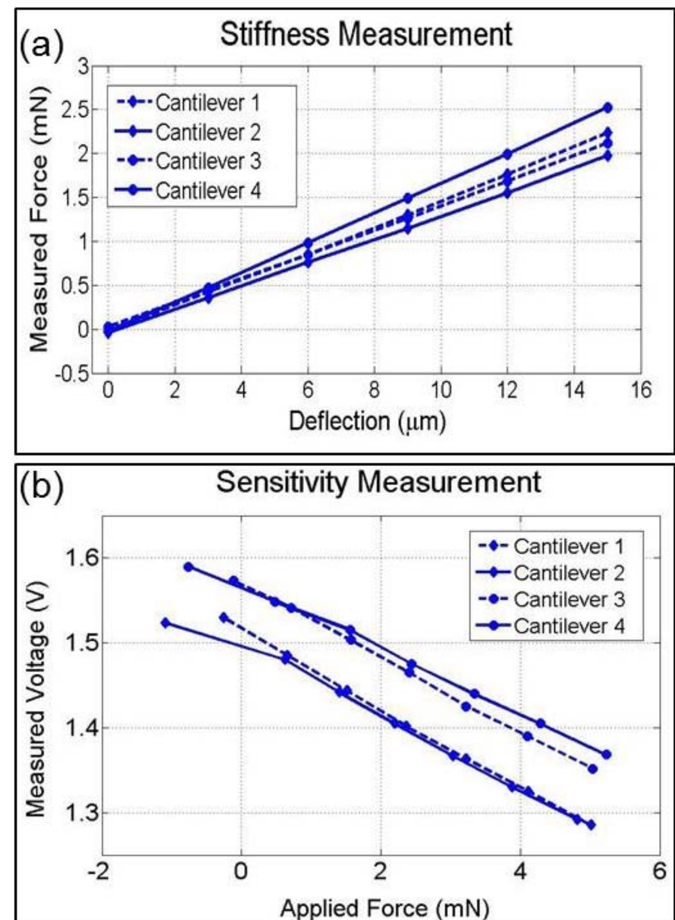

Fig. 10. (a): Graph of measured forces as a function of deflection of (the cantilevers and posts in) the active membrane composite stamp when each of the 4 posts is pressed against the silicon substrate. (b) Graph of measured voltage output from the bridge circuit (for each of the cantilevers) plotted against the applied forces at each of the corresponding posts.

V. CHARACTERIZATION

The individual actuated printing posts are mechanically tested for their stiffness, actuation capabilities and sensitivity. A membrane stamp consisting of 4 post array is mounted into the transfer printing machine. Also mounted on the XY stage of the machine is a 10 gram load cell (Transducer Technique, GSO-10) with a 5 mm polished silicon piece attached to its measuring post. Figure 9 shows the schematic, along with an image of the experimental setup.

First the mounted stamp is interfaced with signal conditioning and drive electronics. The strain gauges on the stamp are connected to Wheatstone bridges, whose output is amplified by a factor of five hundred using an instrumentation amplifier. The amplified signal is then collected using a data acquisition system (National Instruments, USB-6009). The digital signal is then fed into the transfer printer's interface software. The PZT actuators are connected to drive circuits that provide the high voltage for moving the individual posts.

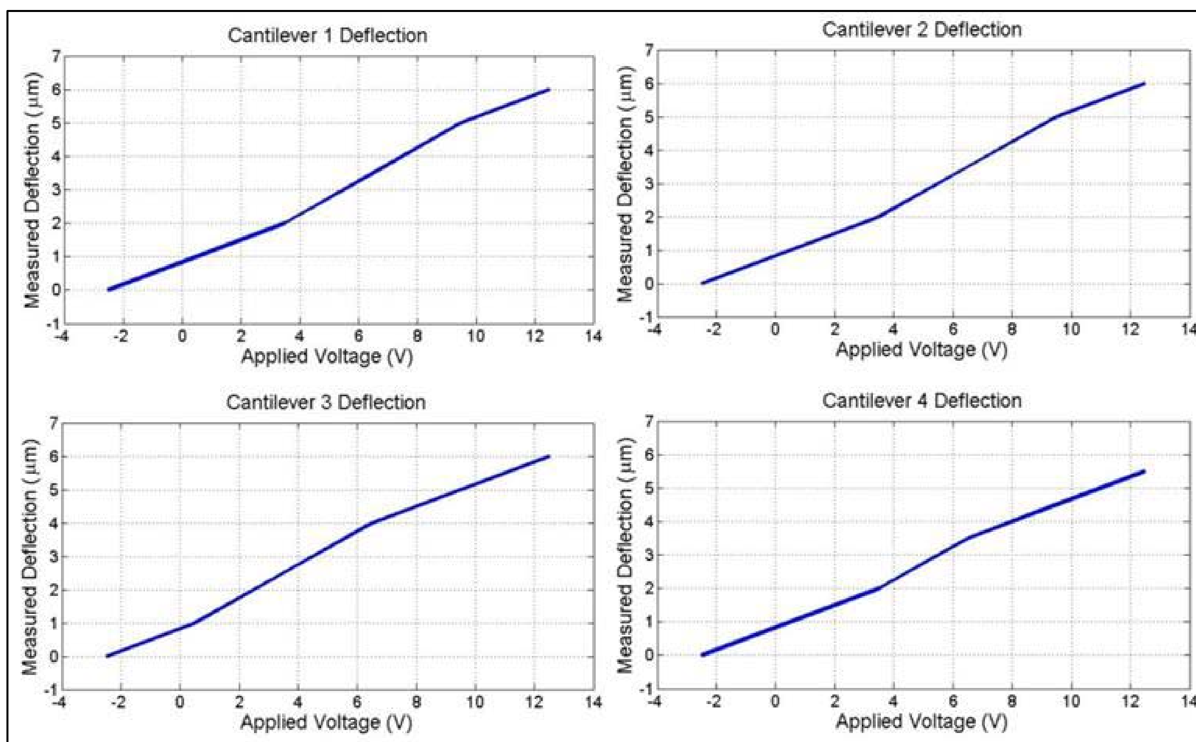

Fig. 11. Measured deflection versus applied voltage graphs for four posts of the active membrane composite stamp. The average measured actuation was 0.4 μm/V.

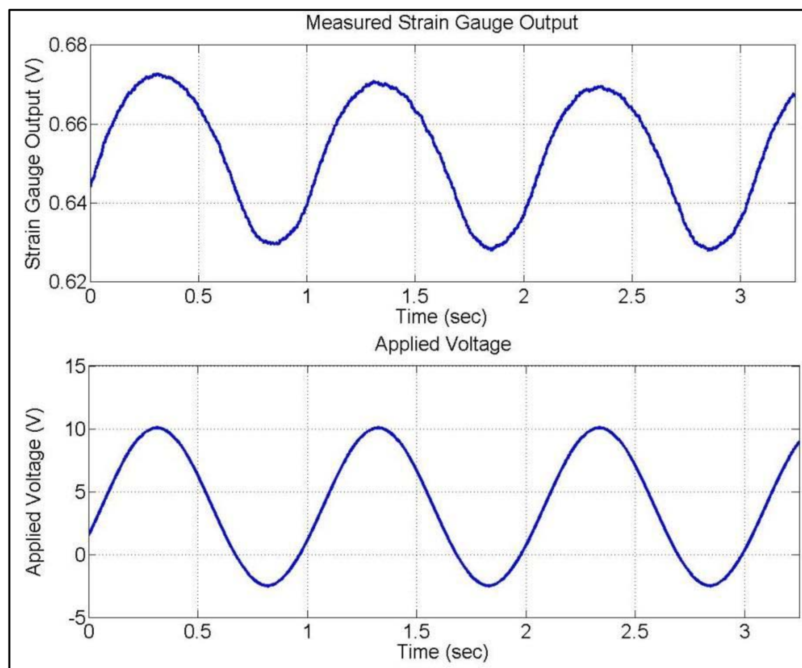

Fig. 12. Strain signal measured using the embedded strain gauge for an applied sine wave with peak-to-peak voltage of 12.5 V and frequency of 1 Hz.

A. *Stiffness Measurement*

To measure the stiffness of the stamp, the post on each of the cantilevers is brought into contact with the silicon attached to the load cell. The z-axis or vertical axis of the printer (to which the stamp is attached) is moved downwards through a known displacement (here 3 micrometers). Because the post and the cantilever in the stamp are the only compliant elements in the set-up, the displacement of the z-axis is accommodated by the local compliance of the stamp obtained as a result of the deflection of the SU-8 cantilever behind the post. Thus, the programmed displacement represents the deflection of the cantilever. The resulting force applied to the load cell is recorded to produce force versus displacement curve for each of the posts of the active membrane composite

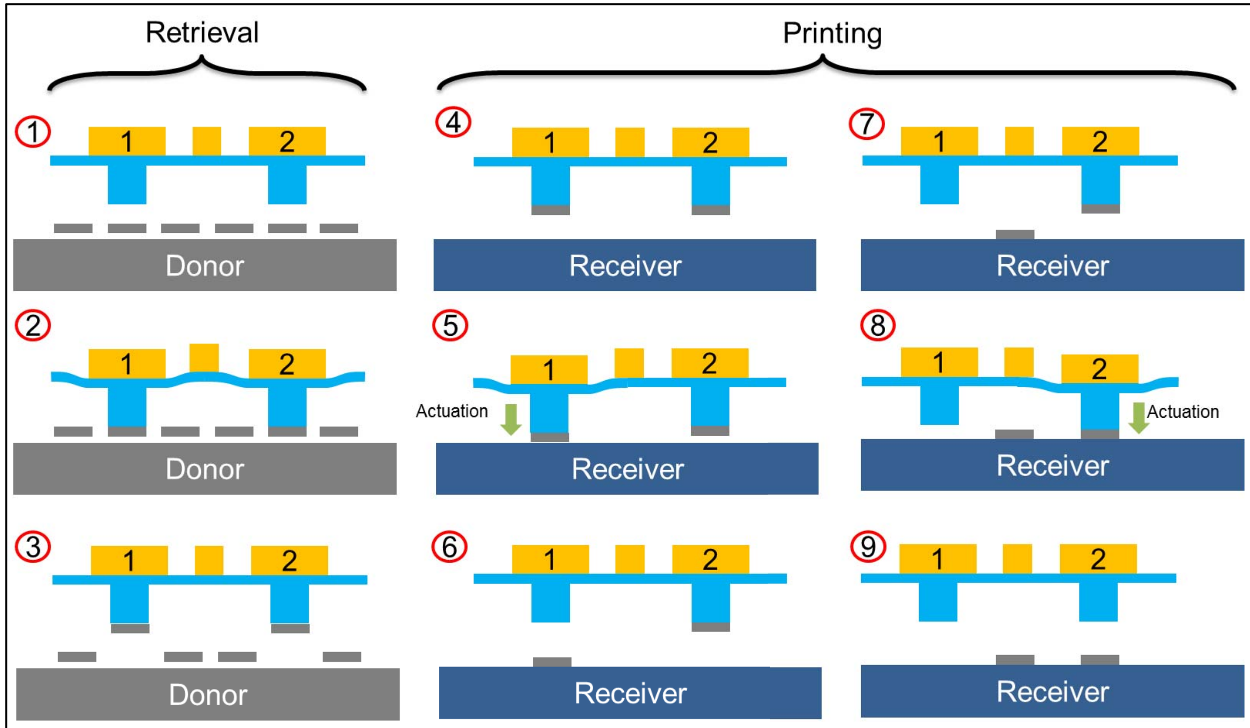

Fig. 13. Schematic representation of micro transfer printing using two posts from an array of four of the active membrane composite stamp. (Steps 1–3) alignment and retrieval of silicon chips from donor wafer. (Steps 4–9) Translation, alignment and selective printing of individual silicon chips; using actuation of individual posts.

stamp in contact with the silicon. Figure 10(a) shows the force-deflection curves for the four posts. Each measurement is repeated 5 times. The average stiffness of the composite cantilever and post structures was measured to be 148.5 N/m with a standard deviation of 13.7 N/m. The measured stiffness is very close to the value of 150 N/m, computed using FEA of the designed stamp.

B. Sensitivity Measurement

During the stiffness measurement, where the stamp is deflected and forces measured, the voltage output from the bridge circuit of the strain gages was also recorded. Using the applied force versus measured output voltage information, the sensitivity of the individual cantilever was calculated. Figure 10(b) shows the force-voltage relationship for the four cantilevers of the array. The average sensitivity was measured to be 42.6 mV/mN with a standard deviation of 0.03 mV/mN.

C. Actuation Measurements

The actuation of the individual posts was also measured during characterization. Voltage is applied to each cantilever and the deflection produced at the PDMS post measured. To measure the deflection, the PDMS post is brought into contact with the Silicon piece attached to the load cell. The location of the z-axis at which contact is detected is recorded as the zero position $\mathbf{Z_0}$. The PDMS post is then moved away from the Silicon by moving the z-axis of the machine. Next a voltage, V, is applied to the piezoelectric actuator and the z-axis of the machine is moved towards the Silicon until contact is detected. This location of the z-axis is recorded as the deflected position $\mathbf{Z_v}$ corresponding to an actuation voltage V. The difference $\mathbf{Z_v}$–$\mathbf{Z_0}$ gives the post's deflection for the applied voltage V. Following this method the deflections for a series of applied voltages are measured. Six different voltages were applied with the magnitude of −2.5, 0.5, 3.5, 6.5, 9.5 and 12.5 Volts. The total deflection measured for this range of inputs was 6 μm. Figure 11 shows graphs of deflection versus applied voltage data collected for the four posts. The measured actuation constant is about 0.4 μm/V, in good agreement with the 0.417μm/V computed from the FEA model of the stamp. The slight difference can be attributed to the actual material properties of the PZT being slightly different (smaller piezoelectric coefficients) from those used in the FEA.

D. Actuation Sensing

The ability of the stamp to sense actuation was also measured as part of the characterization process. Using a function generator a 12.5 V peak-to-peak, 1 Hz sine wave signal was applied to the PZT, to actuate the post. The resulting change in resistance in the strain gauge; due to the strain caused by the actuation, was sensed as a voltage change using the Wheatstone bridge. Figure 12 shows the plot of the waveforms for the collected signal and the applied voltage for a single post. The measured peak-to-peak voltage is 40 mV corresponding to approximately 5 μm deflection of the post.

VI. Transfer Printing Experiment

To demonstrate a practical application of the active membrane composite stamp, it was used to perform selective printing of silicon chips ('ink') in the automated transfer

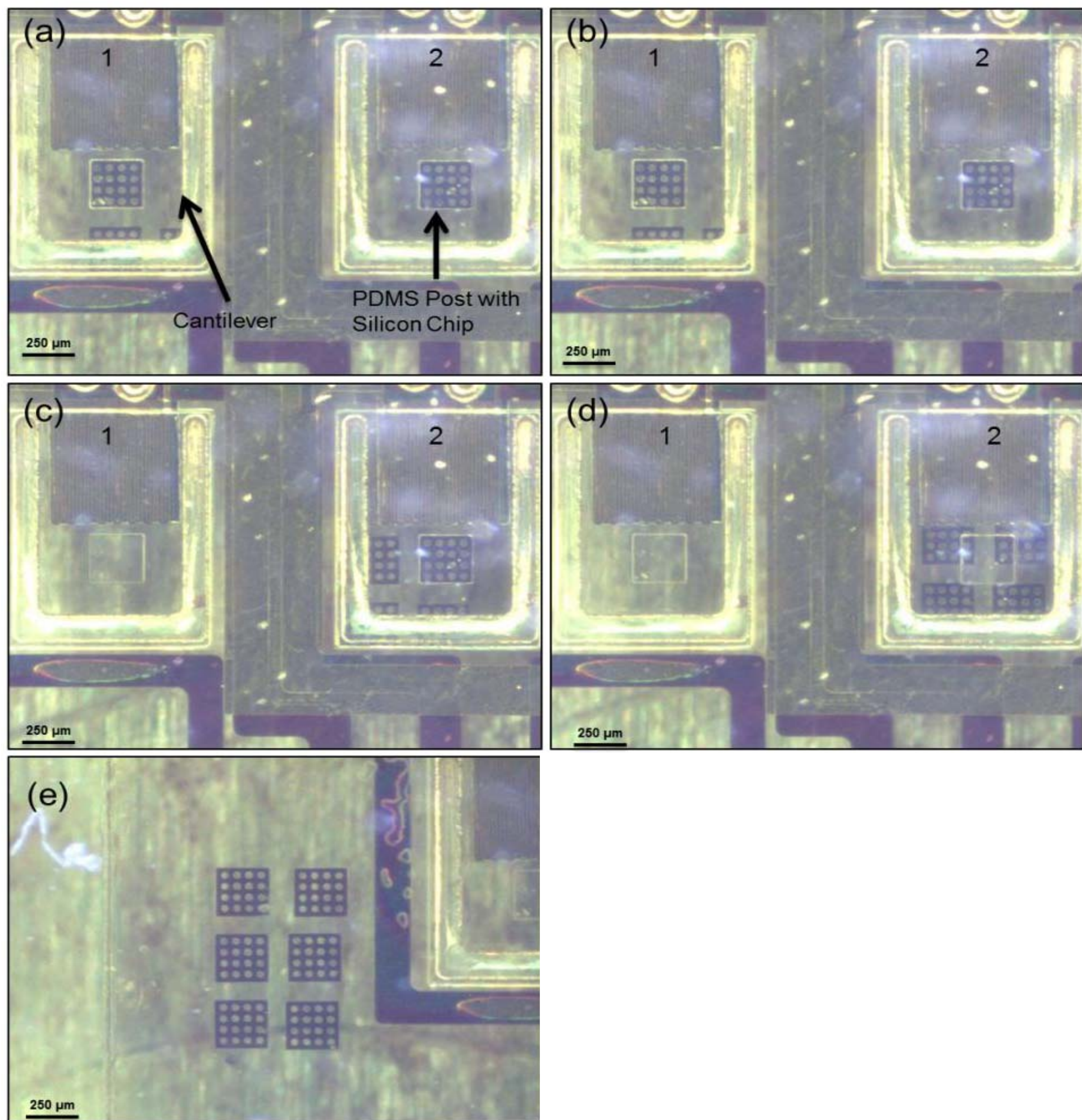

Fig. 14. Image of the active composite cantilever array during transfer printing. (a) Both cantilevers are shown over the receiving substrate with ink attached to their respective PDMS posts. (b) Cantilever '1' actuated and making contact with the substrate surface, (c) image showing the array translated after the silicon chip from cantilever '1' was selectively printed (the PDMS post for cantilever '1' does not have silicon chip attached to it) (d) image showing both cantilevers after successful printing of their respective silicon chips. Also the printed chips can be seen through the cantilevers. (e) Shows the final array with a pitch much smaller than the pitch of the individual cantilevers achieved through selective printing.

printing machine. To perform transfer printing, a single active membrane stamp with 4 posts was mounted onto the transfer printer (to the Z-axis or vertical axis), and two of the posts were interfaced with the drive circuitry. To demonstrate transfer printing we picked up and printed a 2×3 array of silicon squares 250×250 μm and 3 μm thick. The silicon squares have a center to center pitch of 300 μm on the donor wafer. They were picked up by two cantilevers with a pitch of 1500 μm. The silicon chips were selectively printed by actuating the two cantilevers individually and printed at a pitch of 350 μm.

Figure 13 shows a schematic representation of the individual process steps. The process steps are as follows. Step 1 Alignment of the PDMS posts on the cantilevers with the ink. Step 2: Both posts 1 and 2 are actuated before moving the z-axis down to make contact between the PDMS posts and ink. Here only posts 1&2 will make contact and be 'inked'. Posts 3 and 4 remain 'uninked'. Step 3: Retrieval of the ink by posts 1 and 2 when the z-axis is retracted. Step 4: Translation to the receiving substrate. Steps 5&6: Actuation of post 2 brings the first silicon chip in contact with the receiving substrate. Subsequent retraction of the z-axis results in printing

of the first silicon chip. Step 7: Translation of the stamp. Step 8&9: Actuation of post 1 brings second silicon chip in contact with the receiving substrate. Subsequent retraction of the z-axis results in printing of the second silicon chip. After both the chips are printed, the cycle is then repeated starting from step 1.

Figure 14 shows images captured during the course of the experiment. The frames show steps 4 to 9 as represented in Figure 13. Figure 14(a) shows two posts of the active membrane composite stamp with attached silicon chips over the receiving substrate (Figure 13, step 4). Figure 14(b) shows cantilever '1' actuated and contacting the receiving substrate surface. Figure 14(c) shows the two cantilevers after silicon chip from cantilever '1' has been deposited and the array is translated to print with cantilever '2' (Figure 13, step 7). Figure 14(d) shows both cantilevers after their respective chips have been printed (Figure 13, step 9). Figure 14(e) shows the image of the final printed array of silicon chips after the selective printing cycle has been executed 3 times. Notice that the pitch at which the devices were printed is much smaller than the pitch of the cantilevers; resulting in the ability to selectively print ink using the individually actuated cantilevers.

VII. Conclusion

In this paper we presented a novel device architecture and fabrication scheme to create an active polymeric composite membrane. These active membranes provide localized actuation and sensing. These functions are realized by a design strategy that assigns each layer in the membrane different functions. Designed for use as an active stamp in micro-transfer printing, the first layer of the membrane is a functional layer of PDMS, patterned with posts for micro-transfer printing. Next, an actuation layer consisting of thin-film piezoelectric actuators is transfer printed into the composite followed by a SU-8 layer, patterned with cantilevers, whose function is to provide localized compliance for out-of-plane actuation of the posts on the PDMS web. Two metallization layers, one for interconnects and the other for embedding metallic strain gages for sensing along with a patterned handle layer complete the active membrane composite. The stamp is characterized for its stiffness, actuation range and sensitivity and shown to produce around 6 micrometers of motion, sufficient for the micro-transfer printing application. The use of localized out-of-plane actuation in a membrane is demonstrated by designing and successfully executing a selective transfer printing cycle.

The fabrication pathway demonstrates an important and highly scalable approach to microscale heterogeneous integration of polymers, ceramics and metals to realize soft structures with distributed actuation and sensing. Such structures/membranes, besides the demonstrated use as transfer printing stamps can be used in many soft robotic applications. Additionally, the paper demonstrates an important capability for manufacturing where, through heterogeneous integration, one can develop tools to distribute the actuation and sensing so as to get more 'local' monitoring and control in processes that are inherently parallel. In case of micro-transfer printing, the process scales by having stamps with large number of posts that transfer large numbers of 'ink' from the donor to the receiver substrate. We have demonstrated that it is possible to locally control what happens at each post. Our previous work [31] has demonstrated local monitoring of the process at each post, coupled with the actuation capabilities we have now demonstrated, it provides the framework for flexible/selective and robust transfer through local monitoring and control of the process at each post.

References

[1] N. Lu and D.-H. Kim, "Flexible and stretchable electronics paving the way for soft robotics," *Soft Robot.*, vol. 1, no. 1, pp. 53–62, 2014.

[2] C. D. Dimitrakopoulos and P. R. L. Malenfant, "Organic thin film transistors for large area electronics," *Adv. Mater.*, vol. 14, no. 2, pp. 99–117, 2002.

[3] S. R. Forrest, "The path to ubiquitous and low-cost organic electronic appliances on plastic," *Nature*, vol. 428, pp. 911–918, Apr. 2004.

[4] R.-H. Kim *et al.*, "Waterproof AlInGaP optoelectronics on stretchable substrates with applications in biomedicine and robotics," *Nature Mater.*, vol. 9, pp. 929–937, Oct. 2010.

[5] K. J. Lee *et al.*, "Bendable GaN high electron mobility transistors on plastic substrates," *J. Appl. Phys.*, vol. 100, no. 12, p. 124507, 2006.

[6] D.-H. Kim, J. Xiao, J. Song, Y. Huang, and J. A. Rogers, "Stretchable, curvilinear electronics based on inorganic materials," *Adv. Mater.*, vol. 22, no. 19, pp. 2108–2124, May 2010.

[7] D.-H. Kim *et al.*, "Epidermal electronics," *Science*, vol. 33, no. 6044, pp. 838–843, Aug. 2011.

[8] C. Dagdeviren *et al.*, "Transient, biocompatible electronics and energy harvesters based on ZnO," *Small*, vol. 9, no. 20, pp. 3398–3404, 2013.

[9] M. A. Meitl *et al.*, "Transfer printing by kinetic control of adhesion to an elastomeric stamp," *Nature Mater.*, vol. 5, pp. 33–38, Dec. 2006.

[10] D.-H. Kim *et al.*, "Dissolvable films of silk fibroin for ultrathin conformal bio-integrated electronics," *Nature Mater.*, vol. 9, pp. 511–517, Apr. 2010.

[11] J. Kim, S.-H. Bae, and H.-G. Lim, "Micro transfer printing on cellulose electro-active paper," *Smart Mater. Struct.*, vol. 15, no. 3, pp. 889–892, 2006.

[12] A. Wang, W. Chang, A. Murarka, J. H. Lang, and V. Bulovic, "Transfer-printed composite membranes for electrically-tunable organic optical microcavities," in *Proc. IEEE 27th Int. Conf. Micro Electro Mech. Syst.*, San Francisco, CA, USA, Jan. 2014, pp. 1217–1220.

[13] Y. Zhang, H. Keum, K. Park, R. Bashir, and S. Kim, "Micro-masonry of MEMS sensors and actuators," *J. Microelectromech. Syst.*, vol. 23, no. 2, pp. 308–314, Apr. 2014.

[14] T. Komori *et al.*, "Fabrication of Au micro-electrodes on polyimide films using transfer printing techniques," *Appl. Mech. Mater.*, vols. 300–301, pp. 1368–1371, Feb. 2013.

[15] B. Furman *et al.*, "A high concentration photovoltaic module utilizing micro-transfer printing and surface mount technology," in *Proc. 35th IEEE Photovolt. Spec. Conf. (PVSC)*, Jun. 2010, pp. 000475–000480.

[16] S. Burroughs *et al.*, "A new approach for a low cost CPV module design utilizing micro-transfer printing technology," in *Proc. AIP Conf.*, vol. 1277. Freiburg im Breisgau, Germany, 2010, pp. 163–166.

[17] C. A. Bower, E. Menard, S. Bonafede, J. W. Hamer, and R. S. Cok, "Transfer-printed microscale integrated circuits for high performance display backplanes," *IEEE Trans. Compon., Packag., Manuf. Technol.*, vol. 1, no. 12, pp. 1916–1922, Dec. 2011.

[18] J. Im *et al.*, "Direct printing of aligned carbon nanotube patterns for high-performance thin film devices," *Appl. Phys. Lett.*, vol. 94, no. 4, p. 053109, 2009.

[19] J. Mehlich, Y. Miyata, H. Shinohara, and B. J. Ravoo, "Fabrication of a carbon-nanotube-based field-effect transistor by microcontact printing," *Small*, vol. 8, no. 14, pp. 2258–2263, 2012.

[20] H.-P. Lee and W. Ryu, "Wet microcontact printing (μCP) for micro-reservoir drug delivery systems," *Biofabrication*, vol. 5, no. 2, p. 025011, 2013.

[21] C.-E. Ho, C.-C. Chieng, M.-H. Chen, and F.-G. Tseng, "Micro-stamp systems for batch-filling, parallel-spotting, and continuously printing of multiple biosample fluids," *J. Lab. Automat.*, vol. 13, no. 4, pp. 187–197, 2008.

[22] T.-H. Kim *et al.*, "Full-colour quantum dot displays fabricated by transfer printing," *Nature Photon.*, vol. 5, no. 3, pp. 176–182, 2011.

[23] S. Kim *et al.*, "Microstructured elastomeric surfaces with reversible adhesion and examples of their use in deterministic assembly by transfer printing," *Proc. Nat. Acad. Sci. USA*, vol. 107, no. 40, pp. 17095–17100, 2010.

[24] M. S. Kim, J. Park, and B. Choi, "Measurement and analysis of micro-scale adhesion for efficient transfer printing," *J. Appl. Phys.*, vol. 110, no. 2, p. 024911, 2011.

[25] M. B. Tucker, D. R. Hines, and T. Li, "A quality map of transfer printing," *J. Appl. Phys.*, vol. 106, no. 10, pp. 103504-1–103504-8, Nov. 2009.

[26] H.-S. Kim *et al.*, "Unusual strategies for using indium gallium nitride grown on silicon (111) for solid-state lighting," *Proc. Nat. Acad. Sci. USA*, vol. 108, no. 25, pp. 10072–10077, 2011.

[27] K. J. Hsia *et al.*, "Collapse of stamps for soft lithography due to interfacial adhesion," *Appl. Phys. Lett.*, vol. 86, no. 15, p. 154106, 2005.

[28] Y. Y. Huang *et al.*, "Stamp collapse in soft lithography," *Langmuir*, vol. 21, no. 17, pp. 8058–8068, 2005.

[29] N. Ahmed, A. Carlson, J. A. Rogers, and P. M. Ferreira, "Automated micro-transfer printing with cantilevered stamps," *J. Manuf. Process.*, vol. 14, no. 2, pp. 90–97, 2012.

[30] N. Ahmed and P. M. Ferreira, "Transfer printing with microfabricated instrumented stamps," in *Proc. 7th Int. Conf. MicroManuf.*, Evanston, IL, USA, 2012, pp. 354–359.

[31] N. Ahmed, "Towards active monitoring of the micro transfer printing process—MS thesis," M.S. thesis, Univ. Illinois Urbana-Champaign, Urbana, IL, USA, 2011.

[32] S. J. Gross, Q. Q. Zhang, S. Trolier-McKinstry, S. Tadigadapa, and T. N. Jackson, "RF MEMS piezoelectric switch," in *Proc. IEEE Device Res. Conf.*, Salt Lake City, UT, USA, Jun. 2003, pp. 99–100.

[33] S. J. Gross, S. Tadigadapa, T. N. Jackson, S. Troller-McKinstry, and Q. Q. Zhang, "Lead-zirconate-titanate-based piezoelectric micromachined switch," *Appl. Phys. Lett.*, vol. 83, no. 1, pp. 174–176, 2003.

[34] Q. Q. Zhang, S. J. Gross, S. Tadigadpa, T. N. Jackson, F. T. Djuth, and S. Trolier-McKinstry, "Lead zirconate titanate films for d_{33} mode cantilever actuators," *Sens. Actuators A, Phys.*, vol. 105, no. 1, pp. 91–97, 2003.

[35] H. Lorenz, M. Despont, N. Fahrni, N. LaBiance, P. Renaud, and P. Vettiger, "SU-8: A low-cost negative resist for MEMS," *J. Micromech. Microeng.*, vol. 7, no. 3, pp. 121–124, 1997.

[36] eFunda. *Piezo Data: PZT-8*. [Online]. Available: http://www.efunda.com/materials/piezo/material_data/matdata_output.cfm?Material_ID=PZT-8, accessed Apr. 20, 2013.

[37] B. Li, M. Liu, and Q. Chen, "Low-stress ultra-thick SU-8 UV photolithography process for MEMS," *J. Microlithogr., Microfabrication, Microsyst.*, vol. 4, no. 4, p. 043008, 2005.

[38] C. Dagdeviren *et al.*, "Conformal piezoelectric energy harvesting and storage from motions of the heart, lung, and diaphragm," *Proc. Nat. Acad. Sci. USA*, vol. 111, no. 5, pp. 1927–1932, 2014.

Numair Ahmed was born in Pakistan. He received the Bachelor's degree in mechatronics engineering from the National University of Science and Technology, Islamabad, Pakistan, in 2007, and the Master's degree in mechanical engineering from the University of Illinois at Urbana-Champaign, Champaign, IL, USA, in 2011, where he is currently pursuing the Ph.D. degree with the Department of Mechanical Science and Engineering, and is affiliated with the Research Group of Prof. Placid M. Ferreira.

Canan Dagdeviren was born in Istanbul, Turkey, in 1985. She received the B.S. degree in physics engineering from Hacettepe University, Ankara, Turkey, in 2007; the M.S. degree in materials science and engineering from Sabanci University, Istanbul, in 2009; and the Ph.D. degree in materials science and engineering from the University of Illinois at Urbana-Champaign, Champaign, IL, USA, in 2014, as a Fulbright Ph.D. Fellow. She is currently a Post-Doctoral Researcher with the David H. Koch Institute for Integrative Cancer Research and the McGovern Institute for Brain Research, Massachusetts Institute of Technology, Cambridge, MA, USA.

John A. Rogers (F'09) received the B.A. and B.S. degrees in chemistry and physics from the University of Texas at Austin, Austin, TX, USA, in 1989; the S.M. degrees in physics and chemistry from the Massachusetts Institute of Technology (MIT), Cambridge, MA, USA, in 1992; and the Ph.D. degree in physical chemistry, in 1995. From 1995 to 1997, he was a Junior Fellow with the Harvard University Society of Fellows. During this time, he served as the Founder and Director of Active Impulse Systems, Natick, MA, USA, a company that commercialized technologies developed during his Ph.D. work. He joined Bell Labs, Murray Hill, NJ, USA, as a member of the technical staff with the Department of Condensed Matter Physics Research in 1997, where he also served as the Director from 2000 to 2002. He is currently the Swandlund Chair Professor with the Department of Materials Science and Engineering, University of Illinois at Urbana-Champaign, Champaign, IL, USA. He holds joint appointments with the Departments of Chemistry, Bioengineering, Mechanical Science and Engineering, and Electrical and Computer Engineering. He is the Director of the Seitz Materials Research Laboratory and a permanent member of the Center for Advanced Study with the University of Illinois at Urbana-Champaign.

His research includes fundamental and applied aspects of nano and molecular scale fabrication; and materials and patterning techniques for unusual electronic and photonic devices, with an emphasis on bio-integrated and bio-inspired systems. He has authored over 350 papers, and is an inventor on over 80 patents and patent applications; over 50 of which are licensed or in active use by large companies and startups that he has co-founded. His research was recognized with many awards including, most recently, the American Ingenuity Award from *Smithsonian Magazine* (2013), the Robert Henry Thurston Award from the American Society of Mechanical Engineers (2013), the Mid-Career Researcher Award from the Materials Research Society (2013), the Lemelson-MIT Prize (2011), the MacArthur Fellowship from the John D. and Catherine T. MacArthur Foundation (2009), the George Smith Award from the IEEE (2009), the National Security Science and Engineering Faculty Fellowship from the Department of Defense (2008), the Daniel Drucker Eminent Faculty Award from the University of Illinois at Urbana-Champaign (2007), and the Leo Hendrick Baekeland Award from the American Chemical Society (2007). He is a Member of the National Academy of Engineering (2011), and the American Academy of Arts and Sciences (2014). He was a Fellow of the American Physical Society (2006), the Materials Research Society (2007), and the American Association for the Advancement of Science (2008).

Placid M. Ferreira is currently the Head and Tungchao Julia Lu Professor of Mechanical Science and Engineering with the University of Illinois at Urbana-Champaign, Champaign, IL, USA. From 2003 to 2009, he was the Director of the Center for Nanoscale Chemical-Electrical-Mechanical Manufacturing Systems and an NSF-sponsored Nanoscale Science and Engineering Center. He received the Ph.D. degree in industrial engineering from Purdue University, West Lafayette, IN, USA, in 1987; the M.Tech. degree in mechanical engineering from IIT Bombay, Mumbai, India, in 1982; and the B.E. degree mechanical engineering from the University of Bombay, Mumbai, in 1980. He has been with the Faculty of Mechanical Engineering, University of Illinois at Urbana-Champaign, since 1987, where he served as the Associate Head for graduate programs and research from 1999 to 2002.

His research and teaching interests are in the area of precision manufacturing, computer-controlled machine tools, nanomanufacturing, and metrology. He was a recipient of the NSFs Presidential Young Investigator Award in 1990, the Society of Manufacturing Engineers (SME) Outstanding Young Investigator Award in 1991, and the University Scholar Award from the University of Illinois at Urbana-Champaign in 1994. He is also a Fellow of the American Society of Mechanical Engineers and SME. He has served on the Editorial Board of a number of manufacturing-related journals.